Protoplanetary Discs around Low Mass Stars: The effect of the Temperature on the Disc Structure

Adam Parkosidis[1, *]

[1] *Jeremiah Horrocks Institute for Mathematics, Physics & Astronomy, University of Central Lancashire, Preston PR1 2HE, UK*

Planets form in young protoplanetary discs that are made of gas and dust. We simulate locally isothermal gaseous protoplanetary discs evolving around low mass stars using the SPH code "PHANTOM" while varying the disc-to-star mass ratio and the initial exponent of the temperature profile. We investigate different temperature profiles and different disc-to-star mass ratios to estimate the surface density profile of the disc when it reaches the equilibrium state. We refer to the period before this point as the time taken for the discs to relax (approximately few $kyrs$). Each simulation evolves for $5000yr$, which corresponds to 5 orbits of the outer radius of the disc. The disc-to-star mass ratio,w, is set to $0.01, 0.05$ and 0.1, while the temperature profile follows a power law $T_{disc} \propto r^{-q}$(Armitage (2020)). We find that the transport of angular momentum towards the disc outer region is more efficient in colder discs, thus discs with steeper initial temperature profile result to steeper surface density profile when they reach the equilibrium state. Furthermore we find that more massive systems-more massive discs around more massive stars- also result to steeper surface density profile after they have relaxed. Surprisingly, we find that the aforementioned behavior does not apply in the case of the least massive star ($M_\star = 0.2M_\odot$). Furthermore, we see that this discrepancy becomes greater for bigger values of w corresponding to more massive discs around the star.

I. INTRODUCTION

Molecular clouds of gas and dust in the Galaxy collapse under their own gravity when their mass exceeds the Jean mass creating stars with non-zero initial angular momentum and substantial gaseous protostellar discs around them (Shu et al. (1987)). In this early stage, for low mass stars, the disc mass is expected to be comparable to that of the protostar, as a result the self-gravity of the disc should influence the evolution of the system playing an important role in the creation of planets or low mass stars via disc fragmentation (Boss (1997)), as well as affect the accretion of mass onto the protostar's surface. Protostellar discs are also commonly referred as protoplanetary discs and even though there is no strict separation between their definitions, discs with mass comparable to the star mass tend to be referred to as "protostellar", $w \geq 0.1$, while discs with $w < 0.1$ as "protoplanetary".

Protoplanetary discs have masses from $10^{-3}M_\odot$ to $10^{-1}M_\odot$, radii from $10AU$ to 10^3AU and lifetimes less than 10Myr. Such discs are common around PMS stars and are perceived by the strong far-IR/submillimeter radiation they emit, while the accretion of their material onto the central star produces also UV radiation. The evolution of the so called protoplanetary discs is determined by the combined effects of the star's gravity and irradiation, and the angular momentum processes in the disc.

* adam.parkosidis@student.uva.nl

II. HYDRODYNAMIC SIMULATIONS

A. PHANTOM

We carry out different smoothed particle hydrodynamic (SPH) simulations using PHANTOM code (Price et al. (2018)) to evaluate the slope of the surface density profile for locally isothermal gaseous discs after they have reached the relaxed state. The simulations consist of $N = 200,000$ particles initially distributed from $r_{in} = 1AU$ to $r_{out} = 100AU$. We assume that they have the same mass

$$m_i = \frac{M_{disc}}{N} \tag{1}$$

The duration of each simulation is 5000yr corresponding to 5 orbits of the disc outer radius. As the system evolves angular momentum is transferred outwards, while mass inwards. Gas particles that fall within the region of $r < r_{in}$ accreted onto the central star, represented here as a point mass. The viscous evolution process is modeled using the SPH artificial viscosity $a_{AV} = 0.1$ corresponding to discs with

$$a_{SS} = \frac{a_{AV}}{10}\frac{< h >}{H} \tag{2}$$

where a_{SS} is the Shakura & Suynaev parameter (Shakura and Sunyaev (1973), Lodato and Cossins (2011)), H is the scale height and $< h >$ is the mean smoothing length on particles in a cylindrical ring at a given radius. For locally isothermal discs where the temperature of the gas is prescribed as a function of position and assuming an ideal gas, the equation of state is

$$P = \frac{\rho k_\beta T}{\mu m_H} = c_s^2\rho \tag{3}$$

where P is the pressure, ρ the density of the gas and c_s the sound speed. Following (Lodato and Pringle (2007)) the parametrisation of the sound speed c_s is

$$c_s = c_{s,0} R^{-q_c} \tag{4}$$

where $c_{s,0}$ determines the disc thickness (is calculated at a reference radius, in our case $R_{ref} = 10AU$) and the height scale H is

$$H = \frac{c_s}{\Omega_K} = \frac{c_{s,0}}{\sqrt{GM_\star}} R^{\frac{3}{2}-q_c} \tag{5}$$

from which $c_{s,0}$ can easily be determined for a given $R = R_{ref}$. From (3), (4) and (5) the sound speed profile is given by

$$c_s(R) = \sqrt{\frac{k_\beta T_{ref}}{\mu m_H}} R_{ref}^{q_c} R^{-q_c} \tag{6}$$

At this point we performed several test simulations, varying the reference radius between values close to r_{in} and figured out that the result on the slope of the density profile is negligible.

III. INITIAL CONDITIONS

We set the initial disc density, temperature and rotational velocity using information from theoretical models and observations. The temperature and surface density exponents, disc mass and radius and as well as star mass are free parameters. In this section we describe the initial conditions in detail.

A. Disc Volume and Surface Density

Steady-state theory suggests that the surface density of an accretion disc follows a power law of the form $\Sigma(r) \propto r^{-p}$ (Armitage (2020)), where r the distance from the central star on the disc mid-plane. Furthermore, semi-analytical studies of collapsing rotating cloud cores indicate that p is between 1 and $\frac{3}{2}$ (Lin and Pringle (1990)). In our work we assume a surface density profile

$$\Sigma(R) = \Sigma_0 (\frac{R_0^2}{R_0^2 + R^2})^{p/2} \tag{7}$$

where Σ_0 is the surface density at $r = 0$, $R_0 = 10AU$ is the softening radius, which is used to prevent surface density from getting nonphysically large near the star, and R denotes the distance from the star on the disc mid-plane. We note that if $x - y$ is the disc mid-plane then $R = \sqrt{x^2 + y^2}$, while $r = \sqrt{x^2 + y^2 + z^2}$ denotes the distance from the star in three dimensions. In our models we select $p = 2.05$. We compared the initial surface density profile with different values of p to the surface density profile at 1000 years and found that a steeper (higher p) profile matched the relaxed state better. This would mean that the simulation takes less time to reach that relaxed state which is important for us, because discs fragment very quickly (few thousand years) and we can only "trust" the simulation after the disc is relaxed.

The total mass of disc is obtained from

$$M(R) = \int_{R_{in}}^{R_{out}} \Sigma(R) 2\pi R \, dR \tag{8}$$

where there is a gap in the disc around the central star and R_{in} is the inner radius of the disc, while R_{out} is the external one. From (7) and (8) is derived that

$$M_{disc} = \frac{2\pi R_0^2}{2-p} [(\frac{R_0^2 + R_{out}^2}{R_0^2})^{1-\frac{p}{2}}) - (\frac{R_0^2 + R_{in}^2}{R_0^2})^{1-\frac{p}{2}}] \tag{9}$$

The vertical density profile is estimated be taking into account the hydrostatic equilibrium in the direction vertical to the disc mid-plane (z-direction). We assume that the disc is Keplerian and the vertical component of the gravitational acceleration, g_z must balance the vertical pressure gradient

$$\frac{1}{\rho}\frac{dP}{dz} = -g_z = -\Omega^2 z \tag{10}$$

We also consider the effect of self-gravity of the disc, thus we modify (10) and we adopt

$$\frac{1}{\rho}\frac{dP}{dz} = -g_z = -(\frac{G(M_\star + M_{disc}(< R))}{R})z + g_z^D \tag{11}$$

where $M_{disc}(< R)$ is the mass of the disc interior to radius R and g_z the self-gravity of the disc in the z-direction. We therefore assume that the radial component of the disc self gravity can be approximated by considering that the disc mass within radius R is located in the position of the star. From (3), (11) and assuming that the disc is geometrically thin ($z << R$) the volume density of the disc is given by a Gaussian

$$\rho(R, z) = \rho(R, 0) e^{\frac{-z^2}{2H^2}} \tag{12}$$

where $\rho(R, 0)$ is the density midplane and can be calculated from the surface density

$$\Sigma(R) = \int_{-\infty}^{\infty} \rho(R, z) \, dz \; = \sqrt{2\pi} H(R) \rho(R, 0) \tag{13}$$

In case of a self-graviting disc with a central star (Bertin and Lodato (1999)) the scale height $H(R)$ is given by

$$H(R) = \sqrt{\frac{\pi}{8}} \frac{c_s(R)}{\Omega(R)} (\sqrt{\frac{1}{Q(R)^2} + \frac{8}{\pi}} - \frac{1}{Q(R)}) \tag{14}$$

where $Q(R)$ is the Toomre parameter.

Finally, from (12) and (13) we obtain

$$\rho(R, z) = \frac{\Sigma(R)}{\sqrt{2\pi}} \frac{1}{H(R)} e^{\frac{-z^2}{2H(R)^2}} \tag{15}$$

which is the adopted volume density profile for the simulations.

B. Disc Temperature

The two major physical processes that heat the disc are irradiation from the central star and energy generated by viscous dissipation within the disc. Discs that just absorb and re-emit radiation from the central star (*passive discs*) follow a temperature profile $T_d \propto r^{-\frac{3}{4}}$ (assuming a geometrically thin disc, Adams and Shu (1986), Armitage (2020)). Simultaneously, discs that produce heat by viscous dissipation within the disc (*active discs*) also follow a temperature profile $T_d \propto r^{-\frac{3}{4}}$ (Friedjung (1985)). The difference is that for passive discs the luminosity of the central star determines the proportionality constant, while for active discs it is determined by the mass accretion rate and the mass of the central star. However, observations show flatter temperature profiles, which suggest even hotter discs. Kenyon and Hartmann (1987) concluded that this could be explained if discs are flared (the thickness of the disc increases as the distance from the star increases) rather than flat. In that case the temperature profile is not that steep, $T_d \propto r^{-\frac{1}{2}}$, while they showed that in small radii a flared disc temperature profile could be described by $T_d \propto r^{-\frac{3}{4}}$ (isothermal flared disc diverges from the flat solution at $\frac{r}{R_\star} \approx 3$). Other solutions have also been proposed. Natta (1993) pointed out that even a small amount of dust distributed above the disc will scatter considerable amount of radiation back towards the disc mid-plane heating the disc, while Chiang and Goldreich (1997) assumed a model in which outer parts of the disc are optically thin, forming a "disc atmosphere". As a result, dust grains in the atmosphere absorb unattenuated radiation from the star and become hotter, creating a superheated region in the outer regions of the disc. In our work we assume a general profile for the disc temperature

$$T_d(R) = \left(T_0^2 (\frac{R^2 + R_0^2}{AU^2})^{-q} + T_\infty^2 \right)^{\frac{1}{2}} \tag{16}$$

where $R_0 = 0.25AU$ is the softening radius that prevents temperature to be infinitely large close to the center of the star, T_0 is the temperature at $r = 1AU$ (provided that $R_0 << 1AU$, which is generally true), $T_\infty = 10K$ is the temperature far away from the star and from (4), (3) and (16) it is evident that $q = 2q_c$. Beckwith et al. (1990) and Osterloh and Beckwith (1995) observed 81 and 121 young PMS stars in the Tau-Aur dark cloud respectively and found values of q from 0.35 to 0.8. We consider different exponents for our models as q equals to 0.3, 0.5 and 0.7 modifying the disc temperature profile.

C. Disc Rotation

To calculate the initial disc velocity of the disc at distance R we assume that all particles of the disc at the same distance R have the same velocity u, independently of the distance z from the mid-plane. Even though we assumed a Keplerian disc, we slightly modify the equation of the velocity to include the effect of self-gravity

$$u(R) = \left(\frac{G(M_\star + M_{disc}(< R))}{R} \right)^{\frac{1}{2}} \tag{17}$$

where $M_{disc}(< R)$ is the mass of the disc interior to radius R. From (17) it is obvious that a less massive disc tends to rotate with keplerian velocity due to the fact that its self-gravity is negligible compared to the gravity of the star, in contrast a more massive disc rotates faster than a purely keplerian disc, because of the effect of self gravity.

IV. DETERMINATION OF FREE PARAMETERS

First of all we set the initial values for free parameters that are critical for our simulations. More specifically we set the initial mass for the central star, $M_\star$, and the disc, (M_{disc}), based on theoretical models and observations, we also calculate the temperature (T_0) at distance $R = 1AU$ from the star and finally we select the exponent, q, which determines the slope of the disc temperature profile .

At this point we need an estimation about T_0, thus we adopt a very simple model: we assume a flat thin disc in the equatorial plane that absorbs all the incident stellar radiation and re-emits it as a single temperature blackbody, while we neglect other heating processes (e.g energy generated by viscous dissipation within the disc).

The star is assumed to irradiate as a spherical blackbody with $R_\star = 1R_\odot$, thus the flux $F_\star$ passing through its surface is

$$F_\star = \sigma T_\star^4 \tag{18}$$

where σ is *Stefan-Boltzmann constant*, the total intensity for such an emitter is

$$I_\star = \frac{F_\star}{\pi} = \frac{\sigma T_\star^4}{\pi} \tag{19}$$

while the luminosity $L\star$ for a spherical star is

$$L = 4\pi R_\star^2 F_\star \tag{20}$$

Therefore from (18) and (20) we obtain

$$L = 4\pi R_\star^2 \sigma T_\star^4 \tag{21}$$

We also consider a point at an arbitrary distance r from the star, from the point's position, the star subtends a solid angle $\frac{\pi R_\star^2}{r^2}$ (Urry and Padovani (1995)) and the total intensity towards it is $I_\star$. As a result from (19) and (21)

the total flux passing through this surface is

$$F = \frac{1}{4}\int_{\Omega} I_\star \, d\Omega \tag{22}$$

$$F = \frac{1}{4}\frac{\pi R_\star^2}{r^2} I_\star \tag{23}$$

$$16\sigma T(r)^4 = \frac{4\pi R_\star^2}{r^2}\frac{\sigma T_\star^4}{\pi} \tag{24}$$

$$T(r) = \left(\frac{L_\star}{16\pi\sigma r^2}\right)^{1/4} \tag{25}$$

Now we can estimate the luminosity of the star based on the *mass-luminosity relation*, which indicates that

$$\frac{L}{L_\odot} = a\left(\frac{M_\star}{M_\odot}\right)^n \tag{26}$$

with n depending on the mass of the star. Empirical data from observations provide

Initial Mass $M_\odot$	**Index n**	**Constant a**
$0.2 < M_\star < 0.43$	2.5	$a \cong 0.1849$
$0.43 < M_\star < 2$	4.5	$a = 1$
$2 < M_\star < 55$	3	$a \cong 2.8284$

TABLE I: Index n in different mass regimes

while for even bigger stellar masses $n \cong 1$ and $a \cong 3025$ (Prialnik (2010 - 2008)).

Typical values for the disc mass ranging from $10^{-3}M_\odot$ to $10^{-1}M_\odot$. In our work we assume low mass stars, thus from (25) and (26) we calculate the temperature T_0 at distance $r = 1AU$. At this point it is critical to mention that even though the calculation of temperature profile did not derived from sophisticated computations, it is a good enough approximation for our model. The results of our calculations are presented in Table II.

$M_\star\ (M_\odot)$	$L_\star(L_\odot)$	$T_0\ K$
0.2	3.31×10^{-3}	70
0.6	10^{-1}	160
1	1	280

TABLE II: Star related initial input parameter: Mass, Luminosity and Temperature at distance 1 AU

We have now determined the necessary quantities that are implemented in our model. In Table III we present the initial conditions for each simulation.

V. RESULTS

To analyse and visualize the output data of each simulation we use the "Plonk" Python library (Mentiplay (2019)). We present 1-D (Appendix A) and 2-D (Appendix B) illustrations of the surface density of the disc

Run	$M_\star\ (M_\odot)$	$M_{disk}\ (M_\odot)$	w	$T_0\ (K)$	q
1	0.2	0.002	0.01	70	0.3
2	0.2	0.002	0.01	70	0.5
3	0.2	0.002	0.01	70	0.7
4	0.2	0.01	0.05	70	0.3
5	0.2	0.01	0.05	70	0.5
6	0.2	0.01	0.05	70	0.7
7	0.2	0.02	0.1	70	0.3
8	0.2	0.02	0.1	70	0.5
9	0.2	0.02	0.1	70	0.7
10	0.6	0.006	0.01	160	0.3
11	0.6	0.006	0.01	160	0.5
12	0.6	0.006	0.01	160	0.7
13	0.6	0.03	0.05	160	0.3
14	0.6	0.03	0.05	160	0.5
15	0.6	0.03	0.05	160	0.7
16	0.6	0.06	0.1	160	0.3
17	0.6	0.06	0.1	160	0.5
18	0.6	0.06	0.1	160	0.7
19	1	0.01	0.01	280	0.3
20	1	0.01	0.01	280	0.5
21	1	0.01	0.01	280	0.7
22	1	0.05	0.05	280	0.3
23	1	0.05	0.05	280	0.5
24	1	0.05	0.05	280	0.7
25	1	0.1	0.1	280	0.3
26	1	0.1	0.1	280	0.5
27	1	0.1	0.1	280	0.7

TABLE III: The initial conditions of each simulation.

for each simulation in pursuant to Table III. The figures are positioned in 3×3 blocks based on the star mass of the system and every column corresponds to the initial value of the q exponent with $|q| = 0.3, 0.5, 0.7$ respectively. The fitting curve process indicates a power law (Appendix A) for the surface density profile

$$\Sigma(R) = \Sigma_0 R^{-p} \tag{27}$$

and the parameters of the fit are presented in Table IV. Due to the fact that we are interested in the slope of the surface density profile of the disc the 1-D illustrations have been plotted for $20AU < R < 50AU$, where the approximation of a straight line in logarithmic scale is very good. Each graph consists of 100 points, thus the disc has been divided to 100 annuli and each one of them has a width of $0.3AU$. The area A_i of each annulus equals to $A_i = \pi(\frac{R_{i+1}^2 - R_i^2}{2})$, $i = [1, ..., 100]$ & $[R_1 = 20.15AU, R_2 = 20.3AU, ..., R_{100} = 49.85AU$ and the surface density of each annulus is $\Sigma_i = \frac{m N_i}{A_i}$, where m is the mass of each particle (1) and N_i the number of particles in the ith annulus.

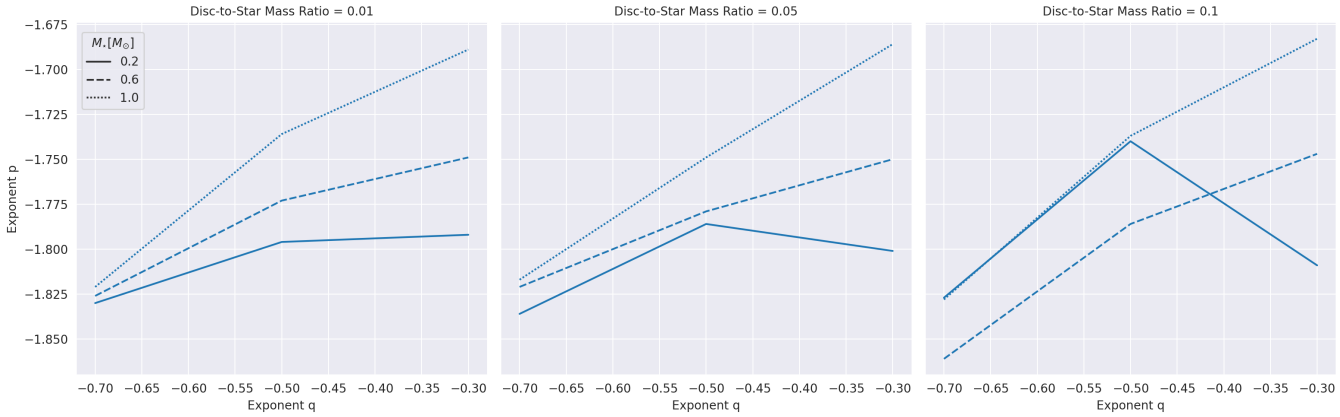

FIG. 1: The exponent of the surface density profile of the disc in relation to the exponent of the temperature profile of the disc for different disc-to-star mass ratios

We first notice that at the beginning of each simulation the initial exponent of the surface density profile (7) was set to 2.05, while now our analysis concludes to $p \in [1.683, 1.861]$ (see Table IV). A lower p corresponds to a flatter surface density profile, which means that the average velocity of gas particles was directed away from the central star, thus part of the gas has been moved to bigger values of R. Of course, a part of the gas was directed towards the central star and eventually accreted onto the star surface. The overall result depicts that in each case the redistribution of angular momentum within the disc leads to a less massive disc with a flatter surface density profile.

Furthermore, focusing on the simulations where the central star is more massive ($M_\star = 0.6$ & $1 M_\odot$) and simultaneously the disc is more massive (see Table III) we observe two things: first, as we choose steeper initial temperature profiles we conclude to also steeper surface density profiles (see Figure 1). The data implies that colder discs transfer angular momentum away more efficiently or equivalently that hotter discs transfer angular momentum away less efficiently. From (5) and (14) someone can notice that a colder disc corresponds to smaller height scale and from (2) this leads to higher values of the Shakura & Suynaev parameter a_{SS}. Consequently, the observed behavior of the disc evolution agrees with our theoretical models. Secondly, a more massive central star and simultaneously a more massive disc results to a flatter surface density profile. In our models, a more massive star means also a more luminous one (26) and that corresponds to a hotter disc (25). However, from (5) and (14) we notice that more massive systems (more massive stars and more massive discs) should have discs rotating faster, thus smaller height scales. The data implies that the contribution of the temperature is more important, but further simulations are necessary to receive safe results.

On the other hand, it is very interesting that in the case of the least massive central star ($M_\star = 0.2\ M_\odot$) the data implies not only that a colder disc does not necessarily transfer angular momentum away more efficiently, but also that a more massive central star and simultaneously a more massive disc does not necessarily result to a flatter surface density profile for the disc; The aforementioned discrepancy is evident in Figure 1, which also illustrates that this deviance becomes greater as the disc mass becomes greater. It is possible that the 5000yr period is a small one for a simulation with such a low mass central star. As mentioned, less massive stars have discs rotating slower, thus the disc around the $0.2M$ star does not necessarily completes 5 orbits. In that case, the disc may have not reached yet the equilibrium state. Further simulations are necessary to investigate in depth the behavior of discs around such low mass stars and to extract safe results.

VI. CONCLUSION AND DISCUSSION

We used the SPH code "PHANTOM" to simulate isothermal gaseous protoplanetary discs evolving around low mass stars, while varying the disc-to-star mass ratio and the initial exponent of the temperature profile,q. For the most massive systems in our sample, where $M_\star = 0.6$ & $1 M_\odot$, we find that as we choose steeper initial temperature profile (colder disc) the transfer of angular momentum towards the limbs of the disc becomes more efficient resulting to steeper surface density profiles. By comparing now the different systems for the same q, the data hints that the more massive, which have more luminous stars based on our model, result to a flatter surface density profile. This implies that the temperature of the disc contributes more importantly than its rotational velocity to the transfer of angular momentum within the disc. Finally, the data do not allow us to safely assume that the aforementioned results also implied in the case

of the least massive central star ($M_\star = 0.2\ M_\odot$).

In future work, more simulations would be necessary to provide further support and confirm that more massive systems, and simultaneously these with more luminous stars, result to flatter disc surface density profiles. Based on the data from the aforementioned simulations, a safer estimation on the importance of the temperature of the disc over its rotational velocity to the transfer of angular momentum within the disc would be possible. Finally, the discrepancy between the results for the least massive system ($M_\star = 0.2\ M_\odot$) and the rest systems ($M_\star = 0.6$ & $1 M_\odot$) seems very interesting. In this very low mass regime ($M_\star \sim 0.2\ M_\odot$), more simulations are necessary before we attempt to argue about the impact of the varying q on the surface density profile of the disc after it has reached the equilibrium state.

VII. ACKNOWLEDGMENTS

I thank Dimitris Stamatellos for the guidance and the helpful discussions. I also thank Adam Fenton for the helpful discussions.

Run	p	$\Sigma_0\ (g/cm^2)$	q
1	1.792 ± 0.014	514 ± 24.11	0.3
2	1.796 ± 0.013	533 ± 23.24	0.5
3	1.830 ± 0.013	622 ± 26.68	0.7
4	1.801 ± 0.013	2616 ± 104.64	0.3
5	1.786 ± 0.016	2535 ± 131.31	0.5
6	1.836 ± 0.014	3110 ± 139.33	0.7
7	1.809 ± 0.016	5263 ± 257.25	0.3
8	1.740 ± 0.017	3875 ± 218.55	0.5
9	1.827 ± 0.012	5934 ± 232.61	0.7
10	1.749 ± 0.017	1358 ± 74.28	0.3
11	1.773 ± 0.013	1526 ± 66.23	0.5
12	1.826 ± 0.012	1868 ± 73.60	0.7
13	1.750 ± 0.014	6689 ± 318.40	0.3
14	1.779 ± 0.014	7668 ± 361.93	0.5
15	1.821 ± 0.013	9043 ± 377.09	0.7
16	1.747 ± 0.014	13019 ± 583.25	0.3
17	1.786 ± 0.013	15491 ± 647.52	0.5
18	1.861 ± 0.013	20621 ± 853.71	0.7
19	1.689 ± 0.016	1816 ± 94.432	0.3
20	1.736 ± 0.015	2251 ± 111.65	0.5
21	1.821 ± 0.011	3070 ± 115.74	0.7
22	1.686 ± 0.017	8861 ± 483.81	0.3
23	1.749 ± 0.014	11545 ± 544.92	0.5
24	1.817 ± 0.012	14999 ± 590.96	0.7
25	1.683 ± 0.017	17281 ± 969.46	0.3
26	1.737 ± 0.015	21821 ± 1108.50	0.5
27	1.828 ± 0.013	30526 ± 1327.88	0.7

TABLE IV: The parameters of the surface density profile and the initial slope of the temperature profile of each simulation

Appendix A - AZIMUTHALLY-AVERAGED SURFACE DENSITY PROFILES

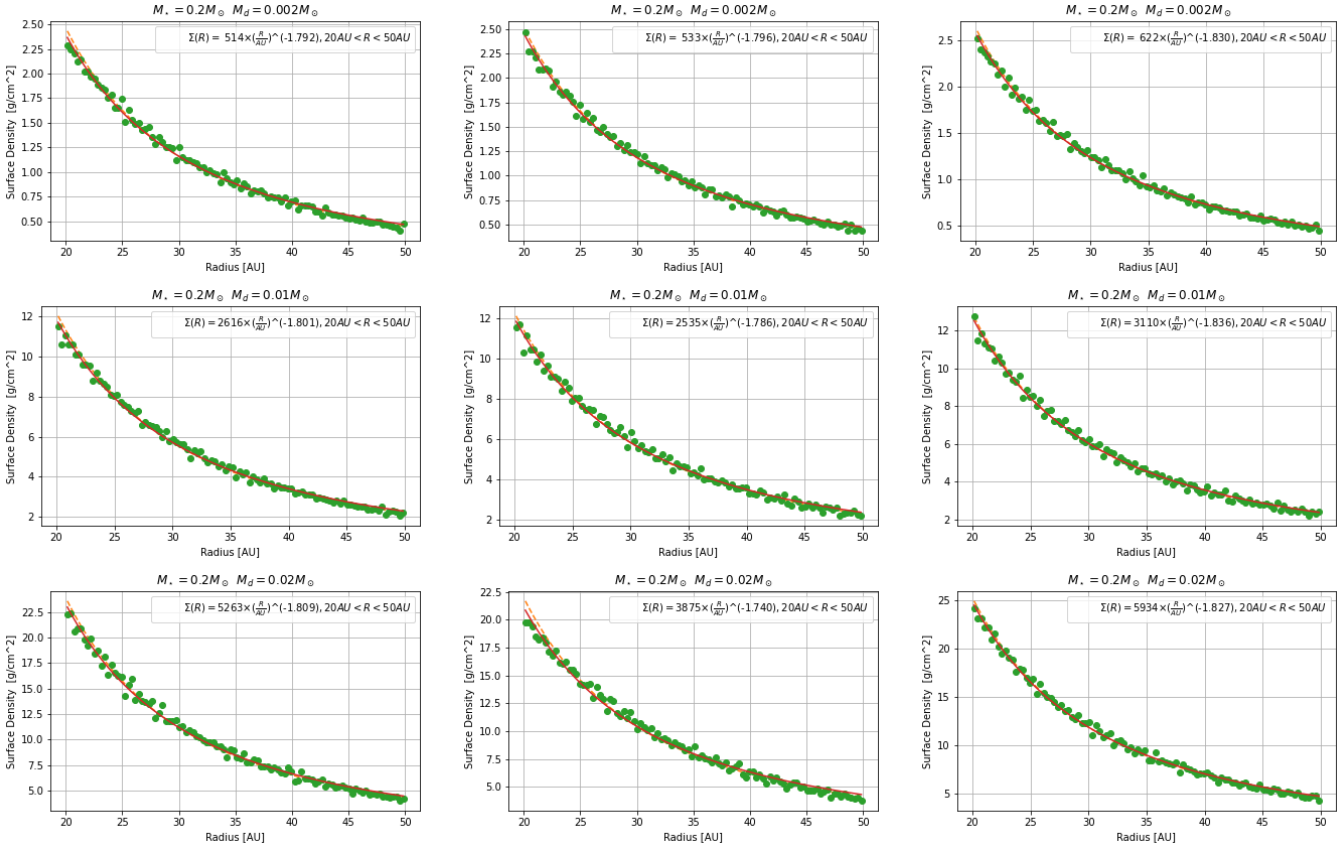

FIG. 2: 1-D Illustrations of the surface density profile of the disc around a $0.2M_\odot$ star after $5000yr$. The disc-to-star mass ratio equals to $0.01, 0.05, 0.1$ for each row respectively, while the initial slope of the temperature profile of the disc equals to $0.3, 0.5, 0.7$ for each column respectively. The disc has reached its relaxed state and the slope of surface density profile has been stabilized. The dashed line show the initial conditions for the fit.

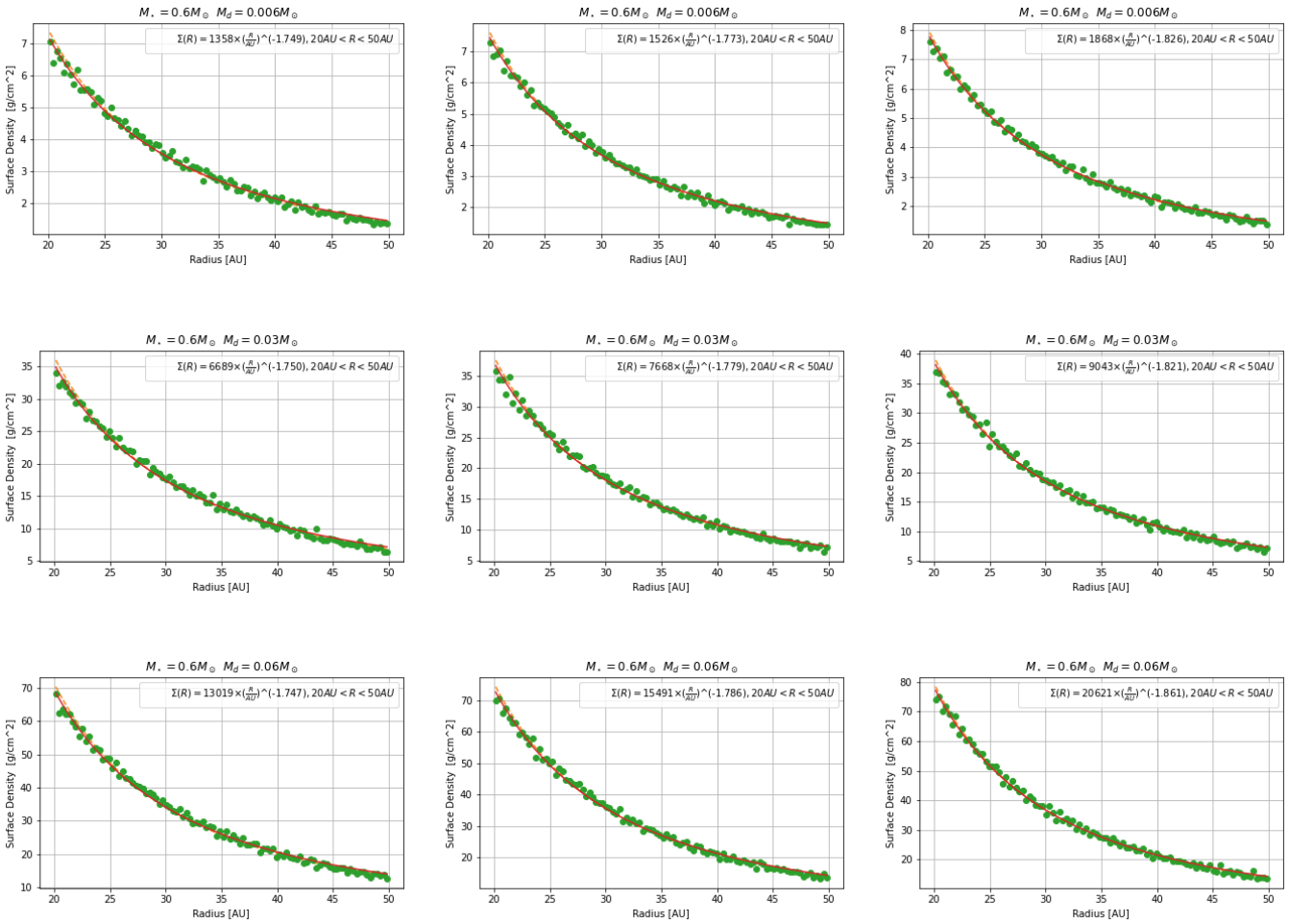

FIG. 3: 1-D Illustrations of the surface density profile of the disc around a $0.6M_\odot$ star after $5000yr$. The disc-to-star mass ratio equals to $0.01, 0.05, 0.1$ for each row respectively, while the initial slope of the temperature profile of the disc equals to $0.3, 0.5, 0.7$ for each column respectively. The disc has reached its relaxed state and the slope of surface density profile has been stabilized. The dashed line show the initial conditions for the fit.

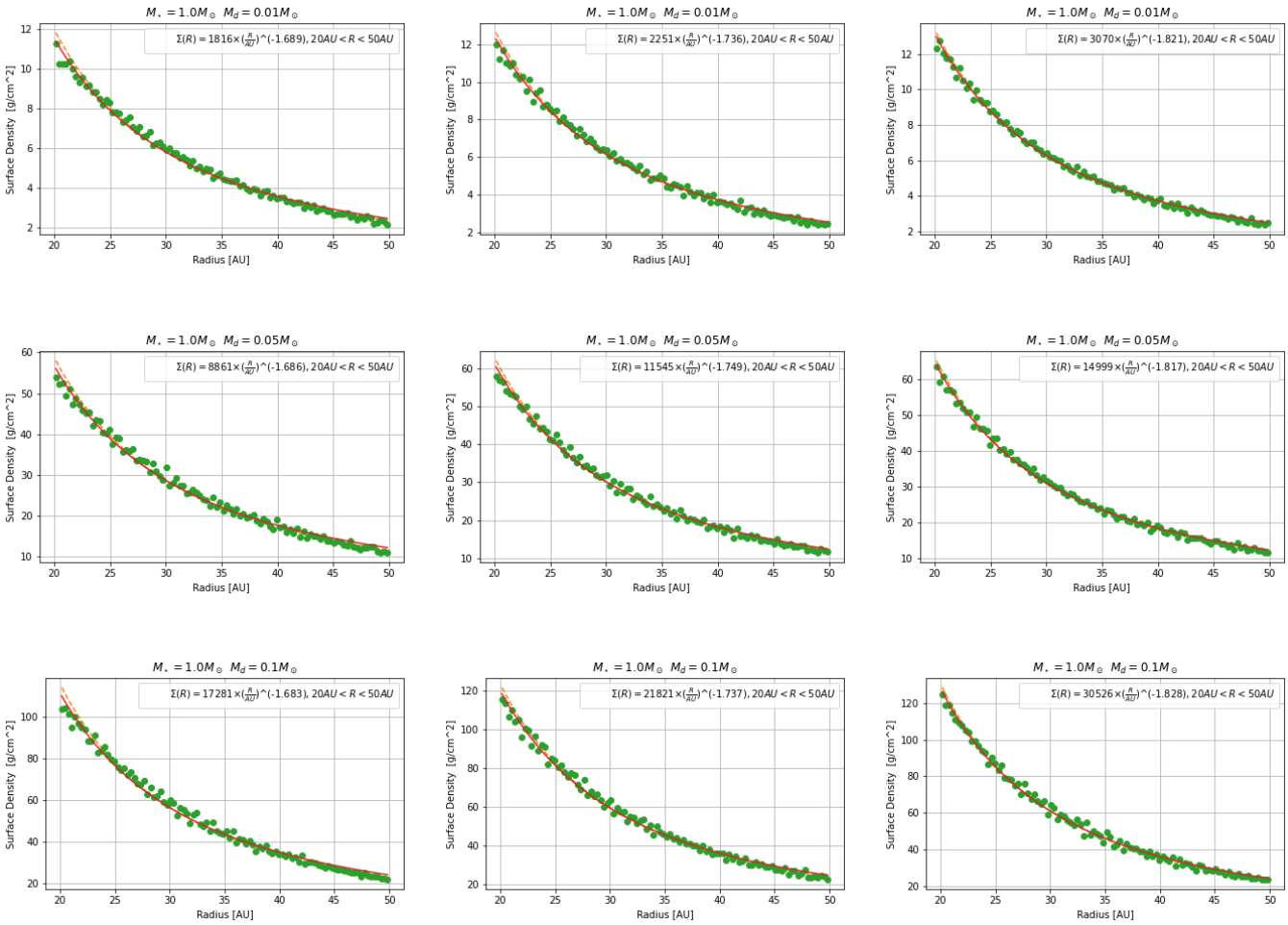

FIG. 4: 1-D Illustrations of the surface density profile of the disc around a $1M_\odot$ star after $5000yr$. The disc-to-star mass ratio equals to $0.01, 0.05, 0.1$ for each row respectively, while the initial slope of the temperature profile of the disc equals to $0.3, 0.5, 0.7$ for each column respectively. The disc has reached its relaxed state and the slope of surface density profile has been stabilized. The dashed line show the initial conditions for the fit.

Appendix B - DISC SURFACE DENSITY

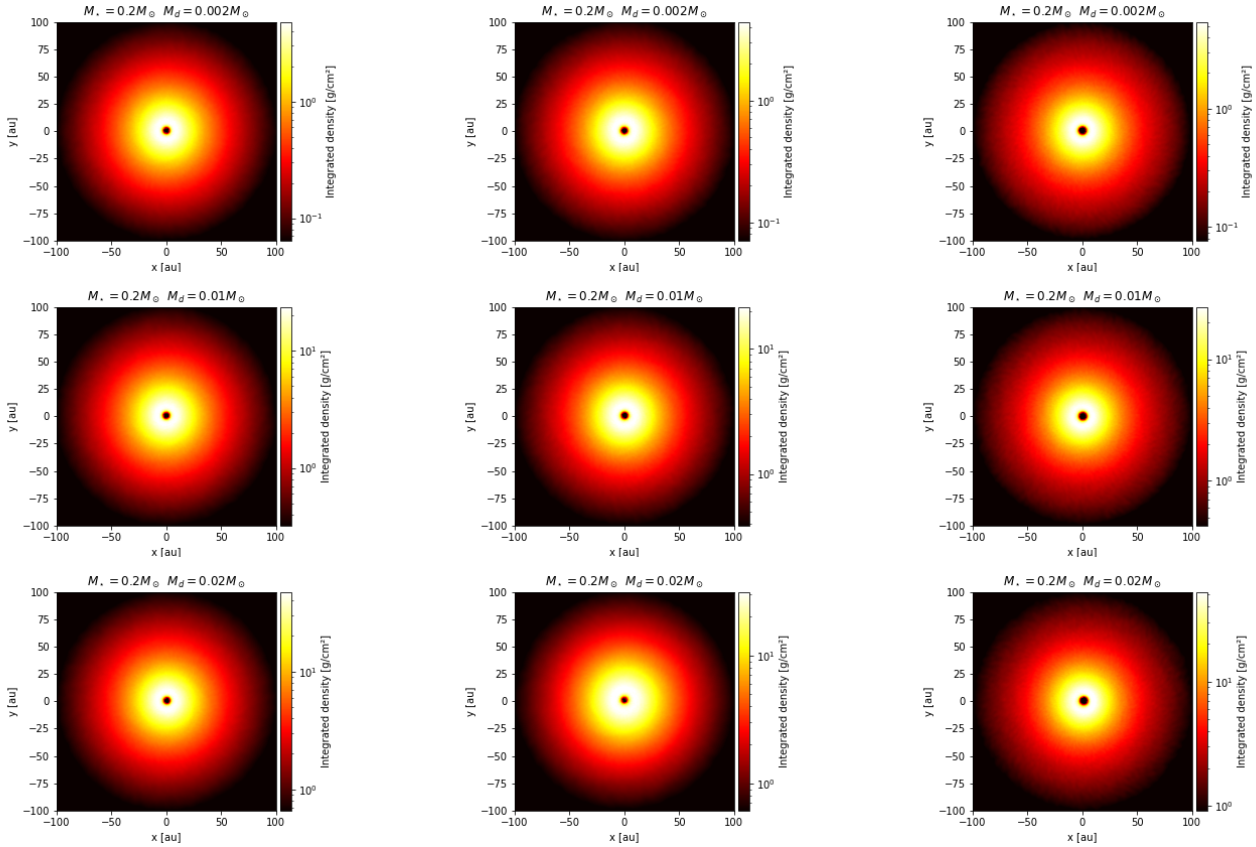

FIG. 5: 2-D Illustrations of the surface density of the disc around a $0.2M_\odot$ star after $5000yr$ - colorbar in logarithmic scale. The disc-to-star mass ratio equals to $0.01, 0.05, 0.1$ for each row respectively, while the initial slope of the temperature profile of the disc equals to $0.3, 0.5, 0.7$ for each column respectively. The disc has reached its relaxed state and the slope of surface density profile has been stabilized

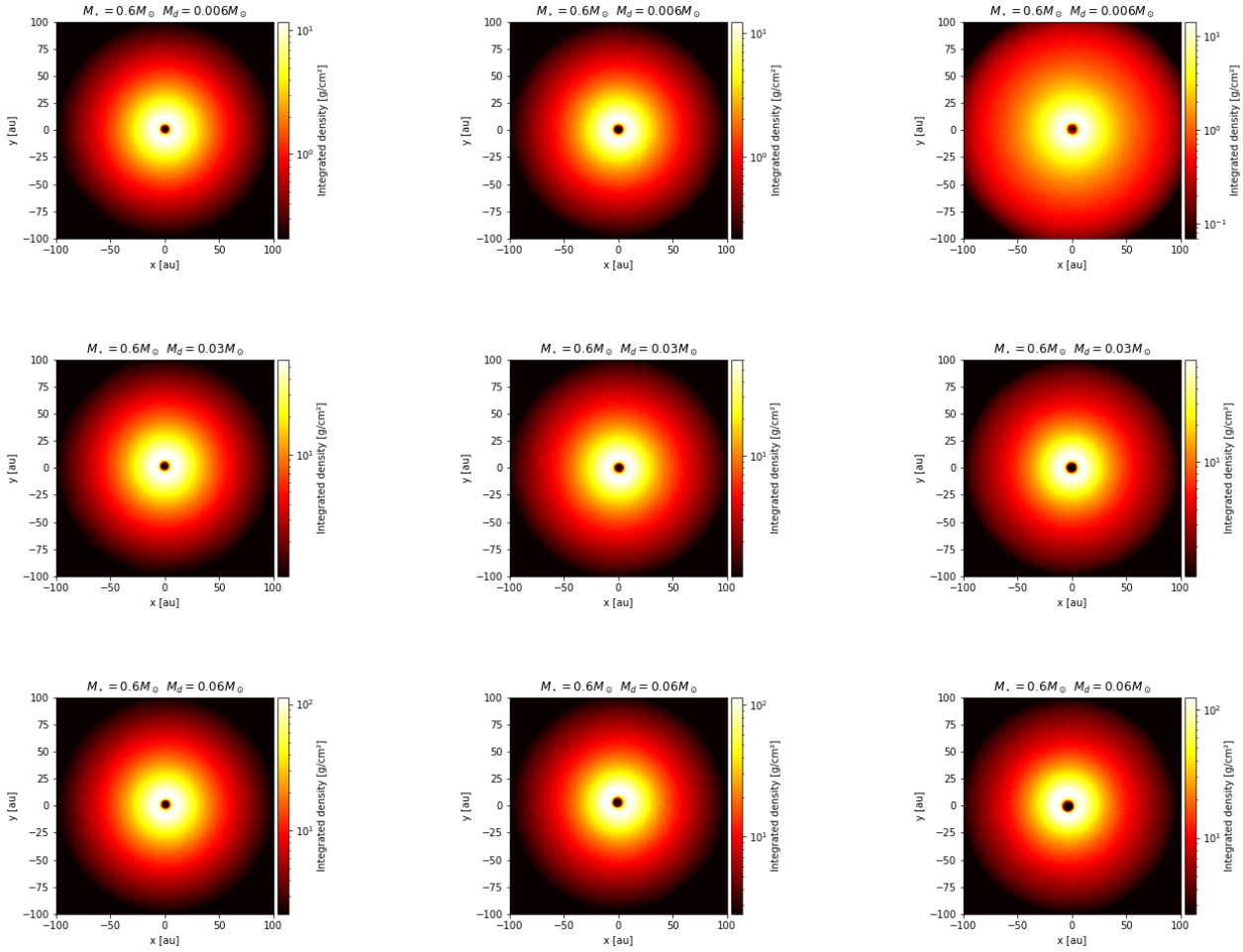

FIG. 6: 2-D Illustrations of the surface density of the disc around a $0.6M_\odot$ star after $5000yr$ - colorbar in logarithmic scale. The disc-to-star mass ratio equals to $0.01, 0.05, 0.1$ for each row respectively, while the initial slope of temperature profile of the disc equals to $0.3, 0.5, 0.7$ for each column respectively. The disc has reached its relaxed state and the slope of surface density profile has been stabilized

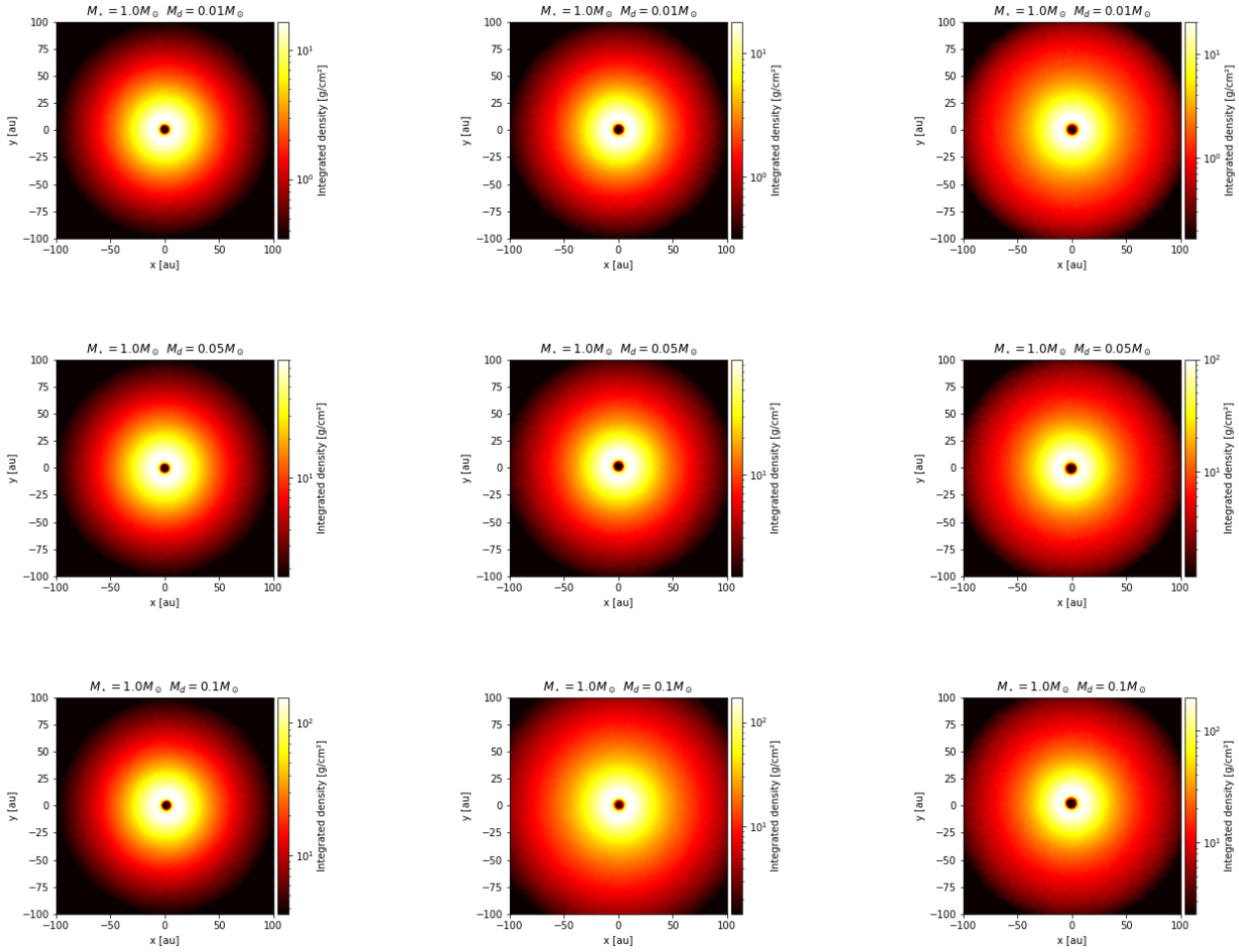

FIG. 7: 2-D Illustrations of the surface density of the disc around a $1M_\odot$ star after $5000yr$ - colorbar in logarithmic scale. The disc-to-star mass ratio equals to $0.01, 0.05, 0.1$ for each row respectively, while the initial slope of the temperature profile of the disc equals to $0.3, 0.5, 0.7$ for each column respectively. The disc has reached its relaxed state and the slope of surface density profile has been stabilized

[1] FC Adams and FH Shu. Infrared spectra of rotating protostars. *The Astrophysical Journal*, 308:836–853, 1986.

[2] Philip J Armitage. *Astrophysics of planet formation*. Cambridge University Press, 2020.

[3] Steven VW Beckwith, Anneila I Sargent, Rolf S Chini, and Rolf Guesten. A survey for circumstellar disks around young stellar objects. *The Astronomical Journal*, 99:924–945, 1990.

[4] G Bertin and G Lodato. Astronomy and astrophysics. 1999.

[5] Alan P Boss. Giant planet formation by gravitational instability. *Science*, 276(5320):1836–1839, 1997.

[6] EI Chiang and P Goldreich. Spectral energy distributions of t tauri stars with passive circumstellar disks. *The Astrophysical Journal*, 490(1):368, 1997.

[7] M Friedjung. Accretion disks heated by luminous central stars. *Astronomy and Astrophysics*, 146:366–368, 1985.

[8] SJ Kenyon and LW Hartmann. Spectral energy distributions of t tauri stars-disk flaring and limits on accretion. *The Astrophysical Journal*, 323:714–733, 1987.

[9] Douglas NC Lin and John E Pringle. The formation and initial evolution of protostellar disks. *The Astrophysical Journal*, 358:515–524, 1990.

[10] G Lodato and PJ Cossins. Smoothed particle hydrodynamics for astrophysical flows. *The European Physical Journal Plus*, 126(4):1–20, 2011.

[11] Giuseppe Lodato and JE Pringle. Warp diffusion in accretion discs: a numerical investigation. *Monthly Notices of the Royal Astronomical Society*, 381(3):1287–1300, 2007.

[12] Daniel Mentiplay. Plonk: Smoothed particle hydrodynamics analysis and visualization with Python. *The Journal of Open Source Software*, 4(44):1884, Dec 2019. doi:10.21105/joss.01884.

[13] Antonella Natta. The temperature profile of t tauri disks. *The Astrophysical Journal*, 412:761–770, 1993.

[14] M Osterloh and SVW Beckwith. Millimeter-wave continuum measurements of young stars. *The Astrophysical Journal*, 439:288–302, 1995.

[15] Dina. Prialnik. *An introduction to the theory of stellar structure and evolution*. Cambridge University Press, Cambridge, 2nd ed. edition, 2010 - 2008. ISBN 9780521866040.

[16] Daniel J Price, James Wurster, Terrence S Tricco, Chris Nixon, Stéven Toupin, Alex Pettitt, Conrad Chan, Daniel Mentiplay, Guillaume Laibe, Simon Glover, et al. Phantom: A smoothed particle hydrodynamics and magnetohydrodynamics code for astrophysics. *Publications of the Astronomical Society of Australia*, 35, 2018.

[17] Ni I Shakura and Rashid Alievich Sunyaev. Black holes in binary systems. observational appearance. *Astronomy and Astrophysics*, 24:337–355, 1973.

[18] Frank H Shu, Fred C Adams, and Susana Lizano. Star formation in molecular clouds: observation and theory. *Annual review of astronomy and astrophysics*, 25(1):23–81, 1987.

[19] C Megan Urry and Paolo Padovani. Unified schemes for radio-loud active galactic nuclei. *Publications of the Astronomical Society of the Pacific*, 107(715):803, 1995.